Journal of Sound and Vibration 329 (2010) 5346–5355

Contents lists available at ScienceDirect

Journal of Sound and Vibration

journal homepage: www.elsevier.com/locate/jsvi

Sound transmission in pipes with porous walls

E. Dokumaci

Department of Mechanical Engineering, Dokuz Eylul University, Izmir, Turkey

ARTICLE INFO

Article history:
Received 9 February 2010
Received in revised form
7 June 2010
Accepted 12 July 2010
Handling Editor: Y. Auregan

ABSTRACT

Pipes with porous (permeable) walls have received the attention of several authors as a noise control element in automotive intake systems; however, a closed theory of sound transmission including the effect of the coupling of the internal and external acoustic fields and the presence of mean flow does not appear to be available. The present paper proposes an integro-differential system for the propagation of plane sound waves in pipes with porous walls, and presents its general numerical solution, as well as an approximate analytical solution. The predicted effect of the coupling between the internal and external acoustic fields in a circular pipe made of reinforced woven fabric walls is shown, and the transmission loss predictions are compared with the existing experimental data in the literature.

1. Introduction

A porous hose made of wire reinforced woven fabric, which is used as a silencing element in automotive intake systems, is a familiar example of a pipe having a porous (permeable) wall. Such pipes are also used in some ventilation and air-handling systems. A model for the transmission of the fundamental mode in a uniform circular pipe with porous wall is presented by Cummings and Kirby [1]. This model neglects the effect of the mean flow, but takes into account the coupling between the in-duct acoustic field and external sound field, which is assumed to be a free-field, by an iterative formulation. The authors also discuss the difficulties encountered in the measurement of the wall impedance, which they eventually use as a tuning parameter to optimize the correlation between the predictions and measurements of sound pressure levels within a specific porous hose. Neglecting the effect of the coupling between the interior and exterior acoustic fields and the presence of mean flow, Park et al. [2] proposed a two-step method for the measurement of the acoustic wall impedance of porous woven hoses without mean flow. In the first step, the wall impedance is measured in a cylindrical apparatus, the resistive part of which is next refined in the second step so that good correlation is achieved with the measured transmission loss of the hose using the reactive part measured in the first step. The effect of uniform mean flow was considered by Park et al. [3], who derived, by neglecting the effect of coupling between the internal and external sound fields, a two-port transfer matrix, which they use in an inverse method for the measurement of the wall impedance of porous woven hoses. In Refs. [2,3], the wall impedance data are presented as function of a parameter called porous frequency. The physics underlying the use of this parameter and its use for the rating of the acoustic properties of the walls of porous woven hoses is discussed by Park et al. [4], who also propose empirical correlations for expressing porous frequency in terms of the flow resistivity of the pipe wall.

The aim of the present paper is to propose a new theory which includes the effects of the coupling between the interior and exterior acoustic fields in the presence of mean flow and present some predictions of the theory for the transmission loss of porous woven hoses. Application of this theory requires knowledge of the pipe wall impedance (it can also be used

E-mail address: dokumaci@deu.edu.tr

0022-460X/$ - see front matter © 2010 Elsevier Ltd. All rights reserved.
doi:10.1016/j.jsv.2010.07.011

for the measurement of the wall impedance, but this is outside the scope of the present analysis). In the present study, the zero mean flow wall impedance correlations published by Park et al. [2] are adopted and the in-duct sound propagation is modeled in the framework of the plane wave theory presented by Dokumaci [5], assuming a sheared parallel mean flow with no-slip flow. The radiation impedance of porous pipe walls is modeled by assuming free-field conditions in the exterior environment and a radiation model based on the solution of Robey [6] for the acoustic radiation from a ring source lying on the surface an infinite cylindrical baffle. Thus, the plane sound wave propagation in the pipe is shown to be governed by linear integro-differential equations and a novel approach is proposed for a rapidly converging numerical solution of these equations to obtain a two-port transfer matrix for a pipe having an arbitrary length. Also presented is an approximate analytical solution, in which the external radiation impedance is represented in a lumped form. Based on these solutions with wall impedance data adopted from Refs. [2], the effect of the coupling between the interior and acoustic fields and the mean flow effects on transmission loss of circular porous woven hoses are discussed. The numerical solution shows that the approximate analytical solution is adequately accurate if the frequency is low enough. The analysis also contains a comparison of the transmission loss prediction of the present theory with the corresponding experimental results given in Ref. [2] for a hose without mean flow and in Ref. [3] with mean flow. The agreement is not perfect, but still fairly satisfactory, despite the fact that the measurement of the wall impedance correlations used are based on duct acoustics theories which are different than the one proposed in this paper.

2. Theory of plane sound waves in pipes with porous walls

Consider a circular infinite uniform pipe embedded in a free-field. This pipe is assumed to be porous-walled in $0 \le x \le L$ and solid impervious-walled everywhere else, where x denotes the pipe axis, and carry isentropic plane sound wave motion superimposed on a sheared parallel mean flow with negligible mean flow through the pipe wall. The continuity and momentum equations for the sound field inside this pipe can be expressed as [5]

$$\frac{1}{c_o^2}\left(-i\omega + v_o\frac{\partial}{\partial x}\right)p + \rho_o\frac{\partial v}{\partial x} = \mu, \tag{1}$$

$$\rho_o\left(-i\omega + v_o\frac{\partial}{\partial x}\right)v + (1+\beta M_o^2)\frac{\partial p}{\partial x} = (w_o - v_o)\mu, \tag{2}$$

respectively. Here, $e^{-i\omega t}$ time dependence is assumed for all the fluctuating quantities, where ω denotes the radian frequency, t the time, i the unit imaginary number; p denotes the acoustic pressure in the pipe, v denotes the axial component of the particle velocity, v_o is the average mean flow velocity over the pipe cross-section, c_o and ρ_o are, respectively, the speed of sound and the mean density of the fluid, w_o is the mean slip flow velocity at the pipe wall, β is a non-dimensional parameter that depends on the mean flow profile, $M_o = v_o/c_o$ is the average mean flow Mach number and μ denotes the fluctuating component of the rate of radial mass inflow into the pipe per unit volume. Since a subsonic low Mach number mean flow is of interest, $\beta M_o^2 \ll 1$ with less than about 1% error [5] and, consequently, this term is neglected in Eq. (2) in the subsequent analysis. The slip velocity, w_o, is kept as a model parameter in the following analysis, although it is eventually assumed to be small compared to v_o to justify the assumption of $w_o/v_o \approx 0$, i.e., no-slip flow, with the boundary layer losses being neglected.

Eqs. (1) and (2) assume that the acoustic pressure and density are isentropically related. This assumption is not strictly true in the presence of sheared mean flow, however, for subsonic low Mach numbers, it provides a sufficiently accurate representation of the linearized energy equation for plane wave motion [5]. On the other hand, in practical applications of porous-walled pipes carrying a mean flow, through flow may be present to some extent depending on the difference between the internal and external ambient pressures. This effect is not included in Eqs. (1) and (2), since it is negligible for the likely through flow rates in practice. It should be noted that, $\mu = 0$ outside the region $0 \le x \le L$, and the solution of Eqs. (1) and (2) for this hard-walled pipe case is given in Ref. [5].

The model adopted here for the acoustic phenomena in a porous wall, presumes uniformly distributed incompressible elementary fluid particles, embedded within the thickness of a rigid pipe wall structure. At any section x, $0 < x < L$, these elementary fluid particles are assumed to be uniformly distributed circumferentially and be free to vibrate with radial velocity $u = u(x)$ under the internal and external acoustic excitation. The mass injection into the unit volume of the pipe due to this radial motion can be expressed as $\mu = -4\rho_o\sigma\, u(x)/D$, where D denotes the internal diameter of the pipe and σ denotes the porosity of the pipe wall. In the present analysis, it will be assumed that the circumferential distribution of the fluid particles is dense enough to be considered as a fluid ring. This assumption, which is approximately valid for a hose made of woven fabric, or if the porosity is large enough, allows a ring-radiation model to be adopted subsequently for the exterior acoustic field.

In the frequency domain, the equation of motion of an elementary fluid particle in a 'ring' of particles at a section x can be expressed as

$$\rho_o c_o \zeta_W u(x) = p(x) - p_e(x), \tag{3}$$

where ζ_W denotes the normalized wall impedance, p_e is the external radiation back-pressure and u is assumed to be positive in the out-of-the-pipe direction. For the present model, p_e can be determined by considering the radiation, to the

exterior acoustic field, from the radially vibrating 'rings' of fluid particles on the surface of the porous-walled region $0 \le x \le L$ on an infinite circular baffle. This problem has been solved by Robey [6] by assuming free-field radiation. This solution is adopted in the present analysis for the calculation of the radiation back-pressure in Eq. (3). Hence, using Robey's equation for the mutual impedance of any two radially vibrating rings axially displaced by an arbitrary distance on an infinite cylindrical baffle, Eq. (3) can be recast as

$$\frac{p(x)}{\rho_o c_o} = \zeta_W u(x) + \int_0^L K(x,\xi) u(\xi)\, d\xi, \tag{4}$$

where

$$K(x,\xi) = \frac{-\mathrm{i}k_o}{\pi} \int_0^\infty \frac{H_0^{(1)}\left(a\sqrt{k_o^2-\lambda^2}\right)\cos\lambda(x-\xi)}{\sqrt{k_o^2-\lambda^2}\, H_1^{(1)}\left(a\sqrt{k_o^2-\lambda^2}\right)}\, d\lambda. \tag{5}$$

Here, $H_j^{(1)}$ denotes the Hankel function of the first kind of order j, a denotes the external radius of the pipe and $k_o = \omega/c_o$ is the wavenumber. Thus, according to the present theory, the plane sound wave propagation in a uniform pipe with porous walls is governed by Eqs. (1), (2) and (4), which constitute a set of coupled linear integro-differential equations.

3. An approximate solution and the exact solution for the case of negligible external radiation back-pressure

An approximate solution of Eqs. (1), (2) and (4) can be derived if the distribution of the radial velocity, $u(x)$, along the length of the pipe is uniform enough to allow the evaluation of the integral in Eq. (4) as

$$\int_0^L K(x,\xi) u(\xi)\, d\xi \approx \zeta_R u(x), \tag{6}$$

where

$$\zeta_R = \int_0^L K(x,\xi)\, dx = \frac{-\mathrm{i}k_o}{\pi} \int_0^\infty \frac{H_0^{(1)}\left(a\sqrt{k_o^2-\lambda^2}\right)\sin(\lambda L)\, d\lambda}{\lambda\sqrt{k_o^2-\lambda^2}\, H_1^{(1)}\left(a\sqrt{k_o^2-\lambda^2}\right)}. \tag{7}$$

Then, from Eqs. (6) and (4)

$$u(x) = \frac{p(x)}{\rho_o c_o(\zeta_W + \zeta_R)}, \tag{8}$$

which indicates that, this approximation is tantamount to the modeling of the free-field radiation impedance of a porous wall by lumped impedance ζ_R. The radiation impedance of porous wall should lump similarly, if the external acoustic field is not a free-field. In general, Eq. (6) should be valid if the length of the pipe is compact enough, that is, if $k_o L \ll 1$, since then the axial distribution of $u(x)$ will be more or less uniform over L, but, the numerical solution of Eqs. (1), (2) and (4) described in the next section shows that it remains adequately accurate for relatively low frequencies larger than the limit indicated by this condition (see Fig. 2). An explanation is provided by Fig. 1, which depicts the spectrum of ζ_R for $L/a = 5$, 50 and the frequency range of 0–1000 Hz, which is usually relevant in automotive intake system applications. It is seen that, for relatively low frequencies, less than about 100 Hz, say, $\zeta_R \approx 0$, implying that the coupling between the internal and exterior acoustic fields is negligible at relatively low frequencies.

Using Eq. (8), Eqs. (1) and (2) can be expressed as, respectively,

$$\left(-\mathrm{i}k_o + \alpha + M_o \frac{\partial}{\partial x}\right) p + \rho_o c_o \frac{\partial v}{\partial x} = 0, \tag{9}$$

$$\rho_o c_o \left(-\mathrm{i}k_o + M_o \frac{\partial}{\partial x}\right) v + \left(-\phi M_o \alpha + \frac{\partial}{\partial x}\right) p = 0, \tag{10}$$

where

$$\phi = 1 - \frac{w_o}{v_o}, \quad \alpha = \frac{4\sigma}{(\zeta_W + \zeta_R)D}. \tag{11}$$

Eqs. (9) and (10) can be solved analytically relatively easily. It is convenient to apply first the transformation:

$$p = p^+ + p^-, \quad \rho_o c_o v = p^+ - p^-. \tag{12}$$

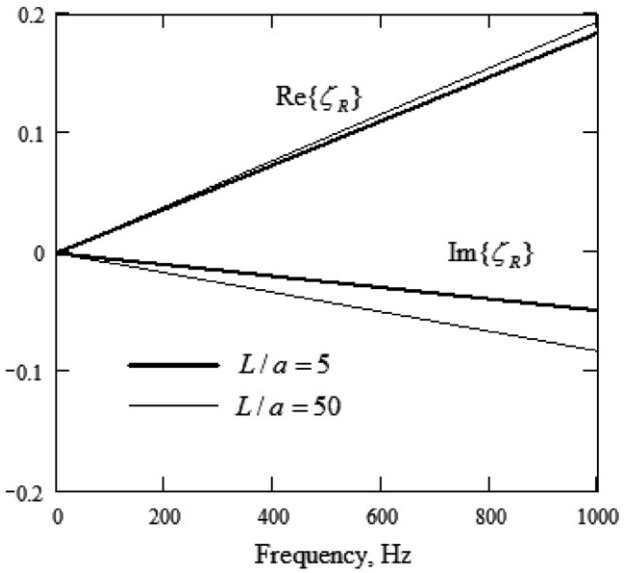

Fig. 1. Lumped normalized radiation impedance of a pipe having porous walls: thick lines, $L/a=5$; thin lines, $L/a=50$.

Then, in matrix notation, Eqs. (9) and (10) become

$$\frac{\partial}{\partial x}\begin{bmatrix} p^+ \\ p^- \end{bmatrix} = \frac{1}{2}\begin{bmatrix} \dfrac{i2k_o+(\phi M_o-1)\alpha}{1+M_o} & \dfrac{(\phi M_o-1)\alpha}{1+M_o} \\ \dfrac{(\phi M_o+1)\alpha}{1-M_o} & \dfrac{-i2k_o+(\phi M_o+1)\alpha}{1-M_o} \end{bmatrix}\begin{bmatrix} p^+ \\ p^- \end{bmatrix}. \tag{13}$$

Invoking the Matrizant theory [7], the general solution of this set of differential equations can be obtained directly in the form of a two-port (four-pole) transfer matrix relationship, namely,

$$\begin{bmatrix} p^+(L) \\ p^-(L) \end{bmatrix} = \mathbf{\Phi}\begin{bmatrix} e^{K^+L} & 0 \\ 0 & e^{K^-L} \end{bmatrix}\mathbf{\Phi}^{-1}\begin{bmatrix} p^+(0) \\ p^-(0) \end{bmatrix}. \tag{14}$$

Here, K^+ and K^- denote the eigenvalues of the square matrix in Eq. (13), which are the wavenumbers of acoustic wave motion in forward (with the mean flow) and backward directions, respectively, multiplied by the unit imaginary number, and $\mathbf{\Phi}$ denotes the modal matrix whose columns are the eigenvectors corresponding to these eigenvalues.

The eigenvalues are

$$K^{\pm} = \frac{\pm ik_o}{1\pm M_o}\frac{\mp M_o \mp \dfrac{i\alpha M_o(1+\phi)}{2k_o} + \sqrt{1-\dfrac{\alpha^2 M_o^2(1+\phi)^2}{4k_o^2}+\dfrac{i\alpha(1+\phi M_o^2)}{k_o}}}{1\mp M_o}. \tag{15}$$

The modal matrix is

$$\mathbf{\Phi} = \begin{bmatrix} 1 & -1+i2\dfrac{k_o+iK^-(1-M_o)}{(1+\phi M_o)\alpha} \\ -1+i2\dfrac{k_o-iK^+(1+M_o)}{(1-\phi M_o)\alpha} & 1 \end{bmatrix}. \tag{16}$$

If the lumped radiation impedance is negligibly small, $\zeta_R \approx 0$, or small enough so that $\zeta_R \ll \zeta_W$ in the second of Eq. (11) for the frequencies of interest, then Eq. (14) becomes the exact solution of Eqs. (1) and (2).

4. The numerical solution

The finite difference method seems to be common in numerical solution of integro-differential equations; however, its usefulness is apt to be limited by slow convergence. The method presented in this section avoids the use of finite differences for differentiation.

Upon applying the transformation of Eq. (12), Eqs. (1) and (2) can be written in matrix form as follows (with $\mu=-4\rho_o\sigma u(x)/D$ and $\beta M_o^2 \ll 1$):

$$\frac{\partial}{\partial x}\begin{bmatrix} p^+ \\ p^- \end{bmatrix} = \mathrm{i}k \begin{bmatrix} \dfrac{1}{1+M_o} & 0 \\ 0 & \dfrac{-1}{1-M_o} \end{bmatrix} \begin{bmatrix} p^+ \\ p^- \end{bmatrix} - \frac{2\sigma\rho_o c_o}{D} \begin{bmatrix} \dfrac{1-\phi M_o}{1+M_o} \\ -\dfrac{1+\phi M_o}{1-M_o} \end{bmatrix} u. \tag{17}$$

Solution of this equation can be expressed as

$$p^{\mp}(x) = e^{\mp \mathrm{i}k_o x/(1\mp M_o)} p^{\mp}(0) + \rho_o c_o \int_0^x g^{\mp}(x,\zeta) u(\zeta)\, d\zeta, \tag{18}$$

where

$$g^{\mp}(x,\zeta) = \frac{\mp 2\sigma(-1\mp\phi M_o)}{D(1\mp M_o)} e^{\mp \mathrm{i}k_o(x-\zeta)/(1\mp M_o)}. \tag{19}$$

Writing Eq.(18) for $n+1$ equidistant points $0=x_0<x_1<x_2<\cdots<x_{n-1}<x_n=L$, $h=x_j-x_{j-1}$, $j=1,2,...,n+1$, and collecting these equations in matrix form gives (the integrals being evaluated by the trapezoid rule)

$$\mathbf{E}^{\mp}\mathbf{P}^{\mp} = \rho_o c_o \mathbf{G}^{\mp}\mathbf{U}, \tag{20}$$

where

$$\mathbf{P}^{\mp} = \begin{bmatrix} p_0^{\mp} \\ p_1^{\mp} \\ \vdots \\ p_n^{\mp} \end{bmatrix}, \quad \mathbf{U} = \begin{bmatrix} u_0 \\ u_1 \\ \vdots \\ u_n \end{bmatrix}, \quad p_j^{\mp} = p^{\mp}(x_j), \quad u_j = u(x_j), \quad j = 0,1,2,\ldots,n, \tag{21}$$

and

$$\mathbf{E}^{\mp} = \begin{bmatrix} -e^{\dfrac{\mp \mathrm{i}k_o x_1}{1\mp M_o}} & 1 & 0 & \cdots & 0 \\ -e^{\dfrac{\mp \mathrm{i}k_o x_2}{1\mp M_o}} & 0 & 1 & \cdots & 0 \\ \vdots & \vdots & \vdots & \ddots & \vdots \\ -e^{\dfrac{\mp \mathrm{i}k_o x_n}{1\mp M_o}} & 0 & 0 & \cdots & 1 \end{bmatrix}, \tag{22}$$

$$\mathbf{G}^{\mp} = h \begin{bmatrix} \frac{1}{2}g^{\mp}(x_1,x_0) & \frac{1}{2}g^{\mp}(x_1,x_1) & 0 & \cdots & 0 \\ \frac{1}{2}g^{\mp}(x_2,x_0) & g^{\mp}(x_2,x_1) & \frac{1}{2}g^{\mp}(x_2,x_2) & \cdots & 0 \\ \vdots & \vdots & \vdots & \ddots & \vdots \\ \frac{1}{2}g^{\mp}(x_n,x_0) & g^{\mp}(x_n,x_1) & g^{\mp}(x_n,x_2) & \cdots & \frac{1}{2}g^{\mp}(x_n,x_n) \end{bmatrix}. \tag{23}$$

Eq. (4) is collocated similarly, by using the trapezoid rule, to obtain

$$\mathbf{P}^+ + \mathbf{P}^- = \rho_o c_o \mathbf{K}\mathbf{U}, \tag{24}$$

where

$$\mathbf{K} = \begin{bmatrix} \zeta_W + \frac{h}{2}K(x_0,x_0) & hK(x_0,x_1) & \cdots & hK(x_0,x_{n-1}) & \frac{h}{2}K(x_0,x_n) \\ \frac{h}{2}K(x_1,x_0) & \zeta_W + hK(x_1,x_1) & \cdots & hK(x_1,x_{n-1}) & \frac{h}{2}K(x_1,x_n) \\ \vdots & \vdots & \vdots & \ddots & \vdots \\ \frac{h}{2}K(x_n,x_0) & hK(x_n,x_1) & \cdots & hK(x_n,x_{n-1}) & \zeta_W + \frac{h}{2}K(x_n,x_n) \end{bmatrix}. \tag{25}$$

Elimination of vector $\mathbf{U}$ from Eqs. (20) and (24) yields

$$\begin{bmatrix} \mathbf{E}^+ - \mathbf{G}^+\mathbf{K}^{-1} & -\mathbf{G}^+\mathbf{K}^{-1} \\ -\mathbf{G}^-\mathbf{K}^{-1} & \mathbf{E}^- - \mathbf{G}^-\mathbf{K}^{-1} \end{bmatrix} \begin{bmatrix} \mathbf{P}^+ \\ \mathbf{P}^- \end{bmatrix} = \mathbf{0}. \tag{26}$$

In this set of $2\times n$ equations there are $2\times n+2$ unknowns. Hence, any unknown can be expressed in terms of any other two unknowns. For example, if the boundary conditions at x_n are given, the pressure wave components at the collocation

points can be determined by arranging Eq. (26) as

$$\begin{bmatrix} p_0^+ \\ \vdots \\ p_{n-1}^+ \\ p_0^- \\ \vdots \\ p_{n-1}^- \end{bmatrix} = \begin{bmatrix} T_{11} & T_{12} \\ \vdots & \vdots \\ T_{n-1,1} & T_{n-1,1} \\ T_{n1} & T_{n2} \\ \vdots & \vdots \\ T_{2n-2,1} & T_{2n,-2,2} \end{bmatrix} \begin{bmatrix} p_n^+ \\ p_n^- \end{bmatrix}. \tag{27}$$

In particular, a porous-walled duct can be introduced as a two-port, or four-pole, acoustic element into a flow duct system using Eq. (27) in the form

$$\begin{bmatrix} p_0^+ \\ p_0^- \end{bmatrix} = \begin{bmatrix} T_{11} & T_{12} \\ T_{n1} & T_{n2} \end{bmatrix} \begin{bmatrix} p_n^+ \\ p_n^- \end{bmatrix}. \tag{28}$$

It should be noted that, this numerical solution is pertinent only when the coupling between the internal and the external acoustic fields is taken into account, as, if otherwise, the exact solution of the problem is given by Eq. (14) with $\zeta_R=0$ in the second of Eq. (11).

5. Transmission loss of woven hoses and discussion

This section presents some predictions of the foregoing theory for the transmission loss (TL) characteristics of porous woven hoses. For a hose of given length, L, internal diameter, D and wall thickness h, the governing parameters are the average mean flow Mach number, M_o, the slip flow parameter, ϕ, the open area porosity of the hose wall, σ, and the normalized wall impedance, ζ_W. The latter is dependent on the other parameters cited, as well as the acoustical and structural properties of the duct wall such as its flow resistance, coating, material composition, roughness and stiffness. However, only a single parameter, commonly called the porous frequency, is used in practice for the rating of porous woven hose characteristics. The porous frequency, f_P, is measured by forcing air flow from the open end and through the walls of a given hose having one end closed, and using the formula [2–4]

$$f_P = \frac{\gamma P_o Q}{2\pi V(P_i - P_o)}, \tag{29}$$

where γ is the ratio of the specific heat coefficients, P_o is the ambient pressure, V is the internal volume of the hose, Q is the volume flux through the hose wall and P_i is the mean pressure at the inlet of the hose. In a consistent system of units, f_P has the unit of s^{-1}, and, hence, the term porous frequency, although this has no physical relation to the usual meaning of frequency. The porous frequency of porous hoses used in automotive intake systems are in the range of about 100–600 s^{-1} [2,3]. It should be noted that, the porous frequency of a given hose is inversely proportional to its length.

In the present study, the measurements presented in Ref. [2] for porous woven hoses without mean flow are used for the wall impedance proper, ζ_W. These measurements give the wall impedance as function of the porous frequency. The curve fitting model proposed in Ref. [2] enables determination of the wall impedance spectra, to the accuracy attainable from the published figures, for a porous frequency range of 100–600 Hz. This correlation, however, cannot be used in the present theoretical model by giving arbitrary values to the porous frequency. This is because, both the present theoretical model and the porous frequency of a given fabric are functions of the duct wall thickness, internal diameter and length, and the values of these parameters should be consistent in both models. To achieve this consistency, the flow resistivity correlation proposed in Ref. [4] is used. For the specific fabric considered in Ref. [4], this correlation gives the following formula, which is adopted in the present calculations, namely,

$$f_P = \frac{2\gamma P_o}{\pi D h}\left(\frac{10^{-6}}{1.358 + 1.259(0.026/\pi DL)}\right). \tag{30}$$

Another parameter of the present theory which is interlinked with the porous frequency is the open area porosity, σ, of the hose wall. But, no information is available about the actual values of this parameter for the fabrics tested in Refs. [2–4]. It is assumed that, the effect of the open area porosity is included in the porous frequency correlations of the wall impedance in some sense so that it can be taken equal to unity, approximately, in the present calculations.

Compared in Fig. 2 are the transmission loss (TL) predictions computed by using the approximate analytical solution, Eq. (14) and the numerical solution described in Section 4, for a 1000 mm long porous hose of internal diameter of 55 mm and wall thickness of 3 mm, for the case of negligible mean flow. The porous frequency of this hose, as computed from Eq. (30), is 350 Hz. Also shown in Fig. 2 is the TL characteristics for the case of negligible radiation impedance, $\zeta_R=0$.

The numerical solution shown in Fig. 2 is computed by using 20 segments. Fig. 3 shows the convergence of this numerical solution in the frequency range considered, as the number of segments is increased. It has been found empirically that, the numerical solution converges for about k_oL number of segments; for example, for the case under consideration, $c_o=344$ m/s and $k_oL=18.3$.

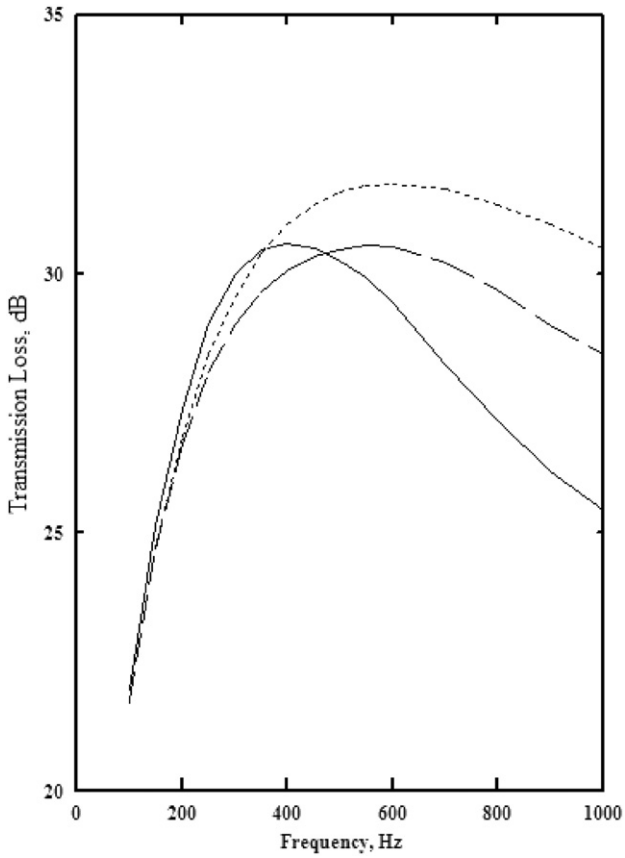

Fig. 2. Predictions of the present theory (solid curve, numerical solution with 20 segments; dashed curve, approximate solution for ζ_R given by Eq. (7); dotted curve: exact solution, ζ_R=0) for the transmission loss of a 1000 mm long porous woven hose having internal diameter of 55 mm, average wall thickness of 3 mm, porous frequency of 350 Hz, and M_o=0, σ=1.

It is seen from Fig. 2 that the approximate solution with the lumped radiation impedance ζ_R given by Eq. (7) and the exact solution for the case of ζ_R=0 are quite close to the numerical solution for relatively lower frequencies. As discussed in Section 3, this indicates that the effect of the coupling between the internal and external acoustic fields is quite small when the frequency is low enough.

In Fig. 4, the TL characteristics of the same porous hose with sheared no-slip mean flow (ϕ=1) of average Mach number M_o=0.1 is compared with the zero mean flow TL spectrum, both predicted by the numerical solution using 20 segments. It should be noted that, sheared no-slip mean flow is physically compatible and consistent with the use of zero mean flow wall impedance.

Next, the TL predictions of the present theory are compared with the corresponding measured values presented by Park et al. [2,3] for 393 and 480 mm long hoses having 55 mm internal diameter and 3 mm average wall thickness. The measured TL spectra are presented in Refs. [2,3] for hoses having porous frequencies of 100, 300 and 500 Hz. In the present study, only the case of the porous frequency of 300 Hz is considered, because, the flow resistivity correlation adopted for the calculation of the porous frequency, Eq. (30), yields reasonable consistency with the average wall thickness of 3 mm only for this porous frequency (3.11 mm for the 480 mm long porous pipe, and 2.97 mm for the 393 mm long porous pipe).

Shown in Fig.5 are the predictions of the present numerical solution with 10 segments, and the exact solution for the case of ζ_R=0, for the transmission loss of the 393 mm long porous woven hose with no mean flow, having 55 mm internal diameter. The experimental points are taken from Ref. [2], to the accuracy attainable from the published figures. The discrepancy between the numerical solution and the measurements is of some concern, but, if the point at 300 Hz is disregarded, the deviations remain within about 1 dB.

Fig. 6 shows the predictions of the present numerical solution, again with 10 segments, for the transmission loss of the 480 mm long porous woven hose carrying a mean flow of average Mach number of 0.058, having 55 mm inside diameter. Results computed by using the present numerical solution with 10 segments and the exact solution for ζ_W=0 are shown for sheared no-slip mean flow (ϕ=1) of average Mach number 0.058. The agreement with the measurements of Ref. [3] is reasonable, and somewhat better than the case of Fig. 5. This provides an experimental confirmation of the physical compatibility of sheared no-slip mean flow model with the zero mean flow wall impedance. It should be noted that, the

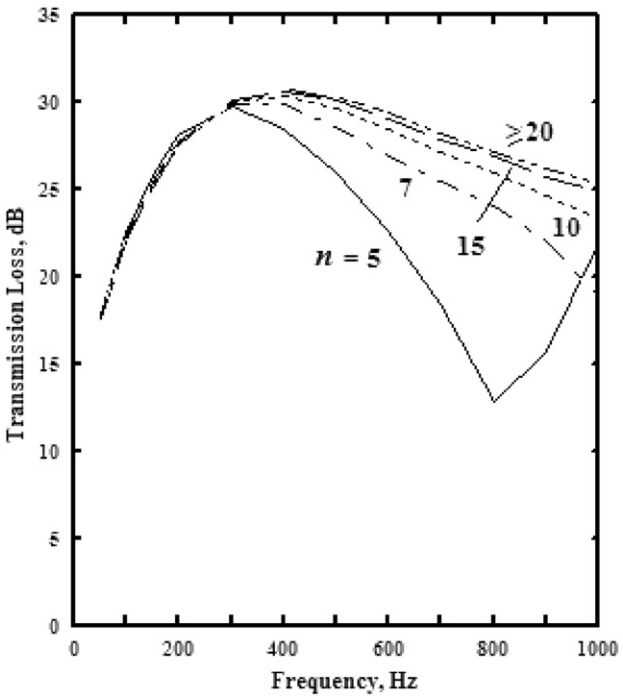

Fig. 3. Convergence of the numerical solution with the number of segments (n) for the transmission loss of porous hose of Fig. 1 (L=1000 mm, D=55, h=3 mm, f_P=350 Hz, M_o=0, σ=1).

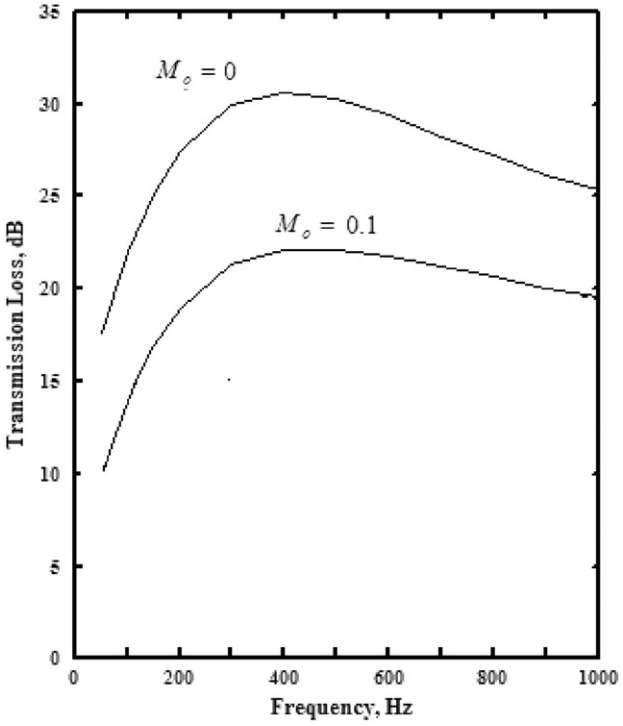

Fig. 4. Effect of the mean flow on the transmission loss of the porous hose of Fig. 1 (L=1000 mm, D=55, h=3 mm, f_P=350 Hz, ϕ=1, σ=1).

commonly made uniform mean flow assumption is avoided, because it is not compatible with the adoption of zero mean flow wall impedance and yields less satisfactory results. Referring to Fig. 6, as ϕ is decreased, the predicted TL spectra move up and the discrepancy with the experimental results becomes worst (1.0–1.5 dB above ϕ=1 spectra) at the limit of

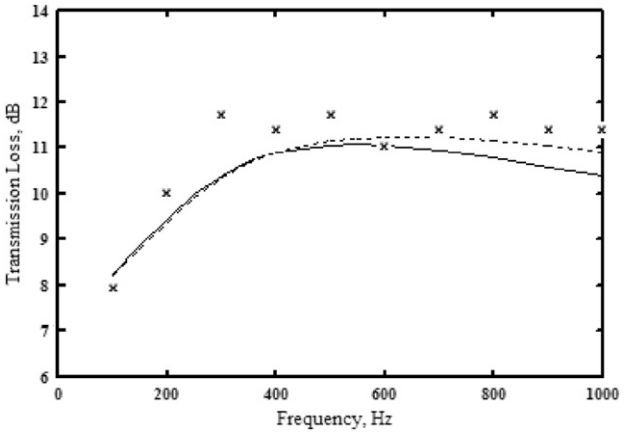

Fig. 5. Transmission loss of a 393 mm long porous woven hose having internal diameter 55 mm, porous frequency of 300 Hz and M_o=0, σ=1. Solid curve: present numerical solution. Dashed curve: present exact solution, ζ_R=0. Marks: measured values [2].

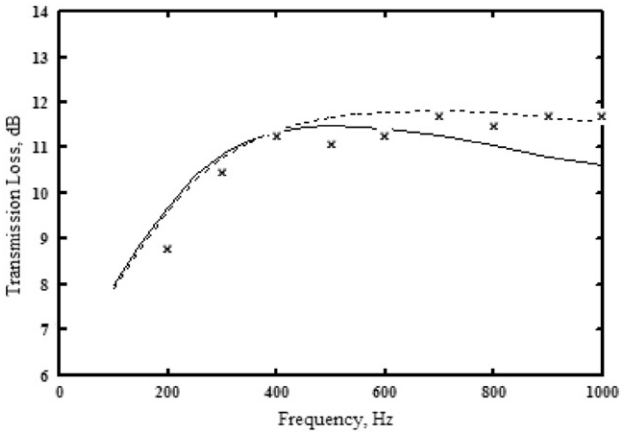

Fig. 6. Transmission loss of a 480 mm long porous woven hose having internal diameter 55 mm, porous frequency 300 Hz and M_o=0.058, ϕ=1, σ=1. Solid curve: present numerical solution. Dashed curve: present exact solution, ζ_R=0. Marks: measured values [3].

uniform mean flow, ϕ=0. Also avoided is the use of wall impedance correlations measured in Ref. [3], since underlying mean flow and turbulent boundary layer model is not consistent with present theoretical model. When these correlations are used for the case of Fig. 6, the shown TL spectra move down by about 2.0 dB for ϕ=0.

A likely source of the discrepancy between the predicted and measured results in Figs. 5 and 6 at relatively high frequencies can be the free-field condition not being exactly applicable in the measurement of the wall impedance correlations. Also, it is observed that, for the relatively higher frequencies, the experimental TL in Figs. 5 and 6 tend to be closer to the present solution for negligible radiation back-pressure. This may be due to the effect of the radiation impedance included to some extent in the measured wall impedance proper, ζ_W, since the measurement method used in Ref. [2] is based on a mathematical model which neglects the effect of the coupling between the interior and exterior acoustic fields.

6. Conclusion

This paper has presented a new theory for the analysis of sound transmission in pipes having porous walls open to an acoustic free-field and demonstrated some of its applications using the zero mean flow wall impedance correlations given in Ref. [2]. A rapidly converging numerical solution is given for the governing integro-differential equations, as well as a simplified approximate solution, which is exact if the coupling between the internal and external acoustic fields is neglected. The predictions of the transmission loss characteristics of a woven hose are in fairly good overall agreement with the existing experimental results, but not to the extent of verifying the predicted effect of the coupling between the internal and external acoustic fields. The present theory can provide a useful basis for experimental identification of this effect. On the other hand, the combination of sheared no-slip mean flow with zero mean flow wall impedance correlation

seems to predict the effect of the mean flow fairly correctly, but verification of this is limited to the case of Fig. 6 and further testing is required to see the general efficacy of this approach.

Eqs. (1) and (2) can be extended for the presence of mean through flow from the walls; however, it should be more practical and of adequate accuracy to include the effect of the mean through flow by dividing the pipe into a number of piecewise-uniform segments and applying the present theory for each segment.

References

[1] A. Cummings, R. Kirby, Low frequency sound transmission in ducts with permeable walls, *Journal of Sound and Vibration* 226 (2) (1999) 237–251.
[2] C.-M. Park, J.-G. Ih, Y. Nakayama, S. Kitahara, Measurement of acoustic impedance and prediction of transmission loss of the porous woven hose in engine intake systems, *Applied Acoustics* 63 (2002) 775–794.
[3] C.-M. Park, J.-G. Ih, Y. Nakayama, H. Takao, Inverse estimation of the acoustic impedance of a porous wowen hose from measured transmission coefficients, *Journal of the Acoustical Society of America* 113 (1) (2003) 128–134.
[4] C.-M. Park, J.-G. Ih, Y. Nakayama, S. Kitahara, Single figure rating of porous woven hoses using a non-linear flow resistance model, *Journal of Sound and Vibration* 257 (2) (2002) 404–410.
[5] E. Dokumaci, Effect of sheared grazing mean flow on acoustic transmission in perforated pipe mufflers, *Journal of Sound and Vibration* 283 (2005) 645–663.
[6] D.H. Robey, On the radiation impedance of an array of finite cylinders, *Journal of the Acoustical Society of America* 27 (4) (1955) 706–710.
[7] R.A. Frazer, W.J. Duncan, A.R. Collar, *Elementary Matrices and Some Applications to Dynamics and Differential Equations*, Cambridge University Press, Cambridge, 1963.